CRINC

REMOTE SENSING LABORATORY

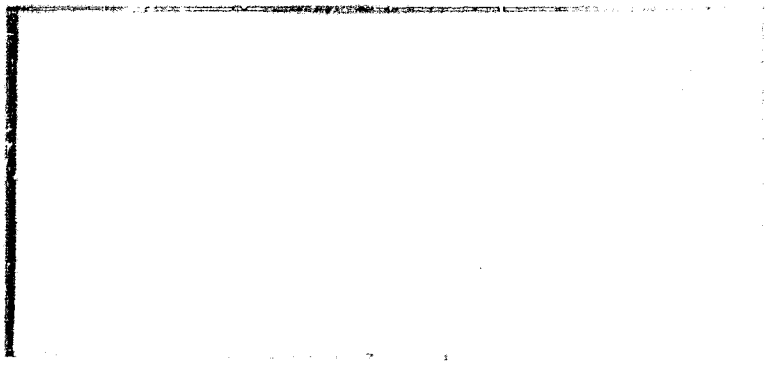

THE UNIVERSITY OF KANSAS CENTER FOR RESEARCH, INC.
2291 Irving Hill Drive—Campus West
Lawrence, Kansas 66045

FOCUSING THE PARABOLIC ANTENNA

L.K. Wu
R.K. Moore
F.T. Ulaby

Remote Sensing Laboratory
The University of Kansas
Center for Research, Inc.
Lawrence, Kansas 66045-2969

RSL Technical Memorandum
RSL TM 587-1

September 1983

Supported by:

NASA GODDARD SPACE FLIGHT CENTER
Greenbelt, Maryland 20771

Contract NAG 5-271

1.0 INTRODUCTION

Both synthetic-aperture antennas and focused-real-aperture antennas can be used to achieve fine resolutions in the across-range dimension of the radar cross-section measurements. Both antenna schemes are achieved by phase error correction. With relative motion between the antenna and target, and digital correction of the phase error, a relatively large aperture size can be synthesized. This gives a narrow antenna beamwidth and, therefore, fine resolution. However, by axially displacing the feed, a quadratic phase distribution is created over the aperture of a parabolic reflector antenna. This produces a plane wavefront over an aperture in the radiating near-field region of the same size as the reflector. The focused parabolic antenna has far-field pattern characteristics in the radiating near-field region. Therefore, it can provide fine resolutions in the across-range dimensions.

The technique of focusing the parabolic antenna is discussed and applied to a 2-1/2-foot parabolic antenna at X-band. The results of the pattern measurements at various ranges from 2.8 m to 5 m are provided.

2.0 REVIEW OF DIFFRACTION INTEGRAL

The pattern at a distance R of a parabolic antenna with an aperture diameter D and focal length f (see Figure 1 for geometry), can be represented by the well-known diffraction integral as [1]

$$I(u) = \int_0^1 F(r)\, e^{-jk\frac{D^2 r^2}{8R}}\, r\, J_0(ur)\, dr \qquad (1)$$

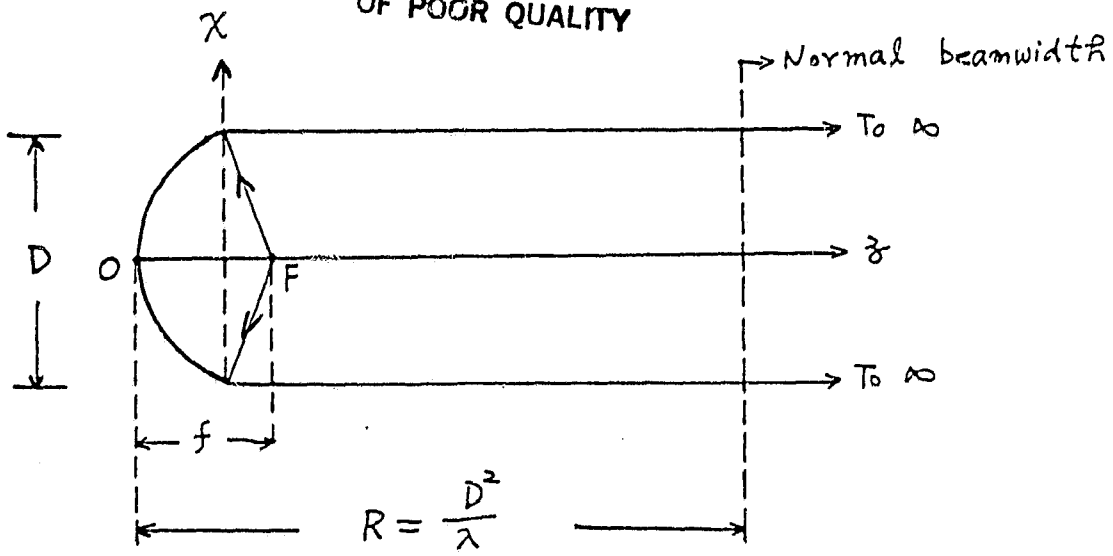

FIGURE 1: Geometry of a Parabolic Antenna Focused at Infinity

where:

r = radius in the aperture normalized to D/2.

u = $(\pi D/2) \sin\theta$, θ is the aspect angle.

F(r) = complex aperture illumination function.

The complex exponential term in (1) is usually referred to as the "Fresnel contribution". This can be treated as an equivalent quadratic phase distribution over the circular aperture, so it dictates the range-dependent variation of the angular pattern of the antenna.

However, for practical purposes, the Fresnel contribution can be ignored and the angular antenna pattern can be treated as range-independent, when the range R exceeds a certain boundary. A loose value of this boundary used in this report is D^2/λ. which corresponds to a maximum phase error of 45° (at the edge of the circular aperture). At this distance, an insignificant degree of the degradation of the pattern characteristics, such as gain reduction and

higher sidelobe level, is expected when compared with that of the far-field pattern at infinity.

3.0 FOCUSING THE PARABOLIC ANTENNA-THEORY

The technique of focusing the parabolic antenna to simulate the far-field pattern in the radiating near-field region has been developed [3-6] because it is desirable to relieve the severe requirement on antenna pattern-measuring ranges for an antenna with a large value of D^2/λ.

As reported in [3] and [4], one can obtain the far-field pattern of the parabolic antenna by axially displacing the feed away from the aperture. The requirement for focusing, for the geometry shown in Figure 2, can be described by [3]

$$r_1 + r_2 = OF'' + OF + \varepsilon \tag{2}$$

For a given focusing range R_ε, the amount of axial displacement of the feed (away from the focal point of the dish) ε can be found as

$$\varepsilon \approx \frac{f^2}{R_\varepsilon}\left[1 + \left(\frac{D}{4f}\right)^2\right] \tag{3}$$

Because of the focusing there exists a region, known as the "depth-of-field" [7], around the focusing range R_ε and bounded by R_{in} and R_{out} as shown in Figure 2, within which the normal far-field pattern is retained. The value of R_{in} and R_{out} are found, for the uniform illumination case, as [3,5]

$$R_{in} = \frac{\frac{D^2}{\lambda}}{1 + \frac{D^2/\lambda}{R_\varepsilon}} \tag{4}$$

and

$$R_{out} = \frac{\frac{D^2}{\lambda}}{-1 + \frac{D^2/\lambda}{R_\varepsilon}} \qquad \text{for } R_\varepsilon < \frac{D^2}{\lambda} \tag{5a}$$

or

$$R_{out} = \infty \qquad \text{for } R_\varepsilon > \frac{D^2}{\lambda} \tag{5b}$$

A detailed derivation of (4) and (5) is given in Appendix I.

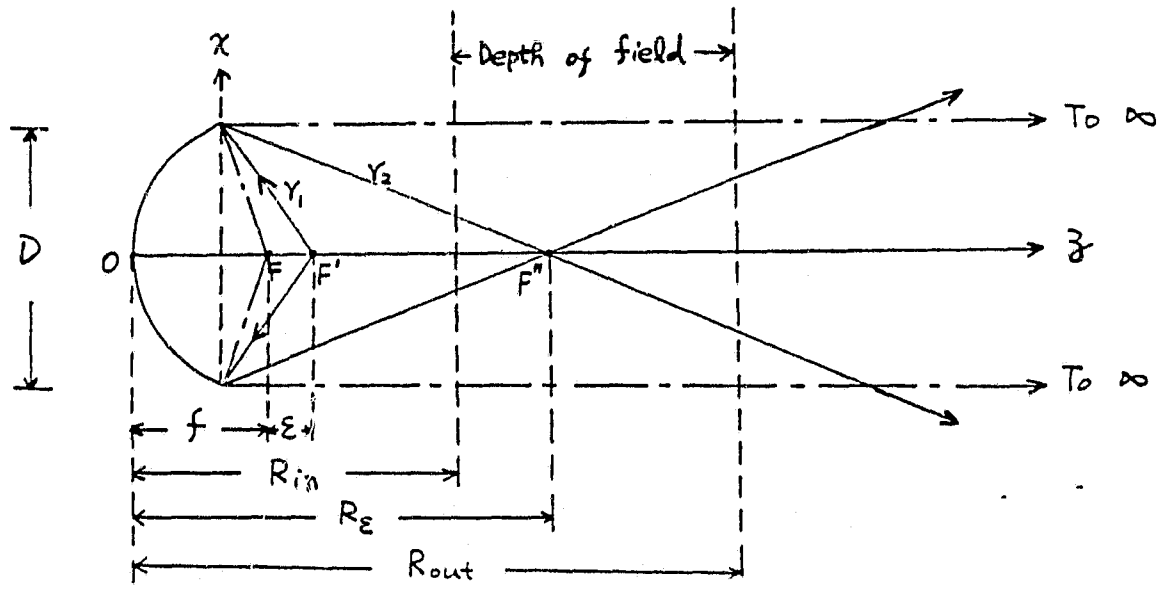

FIGURE 2: Geometry of a Focusing Parabolic Antenna

Note that (3) indicates that the focusing range R_ε depends only on the antenna parameters (f and D) and the amount of feed displacement, but is

independent of the operating freuency. However, R_{in} and R_{out} depend on the frequency)!

4.0 FOCUSING THE PARABOLIC ANTENNA - EXPERIMENT

The parabolic antenna used in the present experiment has the following parameters:

D = 76.2 cm

f/D = 0.34

f = 25.9 cm

ε = 2.85 cm

R_ε = 3.63 m

The measurements were taken at 3 frequencies, which are listed below with the corresponding values of R_{in} and R_{out}:

Frequency GHz	R_{in}, m	R_{out}, m
9.0	3.0	4.59
10.25	3.07	4.44
11.5	3.12	4.34

The actual measurements were taken at the following ranges: 2.8 m, 3.5 m, 4 m, 4.5 m, and 5 m. The results are shown in Appendix II.

The recorded patterns at various ranges provide the following observations: (1) 3 dß beamwidth remains essentially the same; (2) deterioration of the close-in nulls and sidelobes can be observed clearly, and the deterioration worsens as the measuring range is farther away from the focusing range.

5.0 CONCLUSIONS

The theory of focusing a parabolic antenna and its implementation with a 2-1/2-foot dish at X-band were studied. The observed pattern characteristics indicate that this antenna can be used to measure the radar cross-section of targets located in the range of 3 to 5 m away from the antenna.

REFERENCES

[1] Silver, S., Microwave Antenna Theory and Design, New York: McGraw-Hill, 1949.

[2] Bickmore, R.W. and R.C. Hasen, "Antenna Power Densities in the Fresnel Region," Proc. IEEE, vol. 47, December 1959, pp. 2119-2120.

[3] Cheng, D.K. and S.T. Mosley, "On-Axis Defocus Characteristics of the Paraboloidal Reflector," Trans. IRE, AP-3, October 1955, pp. 214-216.

[4] Bickmore, R.W., "On Focusing Electromagnetic Radiator," Can. J. Phys., vol. 35, 1975, pp. 1292-1298.

[5] Bickmore, R.W., "Fraunhofer Pattern Measurement in the Fresnel Region," Can. J. Phys., vol. 35, 1975, pp. 1299-1308.

[6] Johnson, R.C., H.A. Ecker and J.S. Hollis, "Determination of Far-Field Antenna Patterns from Near-Field Measurements," Proc. IEEE, vol. 61, December 1973, pp. 1668-1694.

[7] Hansen, R.C., Microwave Scanning Antennas, vol. 1, Academic Press, 1964, pp. 40-46.

APPENDIX I:

DERIVATION OF R_{in} AND R_{out}

Displacing the feed away from the focal point results in path length differences for the rays, emerging from the feed, which get reflected back to the aperture. The difference along the radial dimension of the aperture is given by:

$$\delta = -2\varepsilon \left[1 - \frac{r^2}{\left(\frac{4f}{D}\right)^2 + r^2}\right] \qquad \text{(A1.1)}$$

By realizing that $0 < r < 1$ and $f/D \geq 0.25$, one can approximate (A1.1) as

$$\delta \approx -2\varepsilon \left[1 - \frac{r^2}{\left(\frac{4f}{D}\right)^2 + 1}\right] \qquad \text{(A1.2)}$$

Substituting (A1.2) back into (1), we have

$$I(u) = \int_0^1 F(r)\, e^{jk\left(\delta - \frac{D^2 r^2}{8R}\right)}\, rJ_0(ur)\, dr \qquad \text{(A1.3)}$$

To solve (A1.3), we proceed as follows. First,

$$k\delta = \left(\frac{2\pi}{\lambda}\right)(-2\varepsilon)\left[1 - \frac{r^2}{\left(\frac{4f}{D}\right)^2 + 1}\right] = \frac{-4\pi\varepsilon}{\lambda} + \pi r^2 \frac{4\varepsilon}{\lambda\left[\left(\frac{4f}{D}\right)^2 + 1\right]} \qquad \text{(A1.4)}$$

using (3), we have

$$\frac{\varepsilon}{\lambda} = \frac{f^2}{R_\varepsilon \lambda}\left[1 + \left(\frac{D}{4F}\right)^2\right] = \frac{D^2/\lambda}{16R_\varepsilon}\left[\left(\frac{4f}{D}\right)^2 + 1\right] \qquad \text{(A1.5)}$$

(A1.5) indicates that, for given antenna parameters and focusing range, ε/λ is a constant. Therefore, one can ignore (within the integral) the first term on the right-hand side of (A1.4), and (A1.4) becomes

$$k\delta = \pi r^2 \frac{4\varepsilon}{\lambda[(\frac{4f}{D})^2 + 1]} = \frac{\pi r^2}{4} \frac{D^2/\lambda}{R_\varepsilon} \tag{A1.6}$$

Applying the result given above, we can rearrange the parameter of the complex exponential term in (A1.3) as follows:

$$k(\delta - \frac{D^2 r^2}{8R}) = \frac{\pi r^2}{4} \frac{D^2/\lambda}{R_\varepsilon} - \frac{2\pi}{\lambda} \frac{D^2 r^2}{8R} = B \frac{\pi r^2}{4} \tag{A1.7}$$

where

$$B = \frac{D^2}{\lambda} (\frac{1}{R_\varepsilon} - \frac{1}{R}) \tag{A1.8}$$

Now, one can write (A1.3) as

$$I(u) = \int_0^1 F(r)\, e^{jB\frac{\pi r^2}{4}}\, rJ_0(ur)\, dr \tag{A1.9}$$

which clearly indicates the analogy (and thus the variation of the pattern characteristics) between the focused and unfocused (as focused at infinity) parabolic antenna.

Upon applying the far-field requirement for the unfocused dish, namely, maximum phase error not to exceed 45° ($\pi/4$) at the edge of the aperture (r=1), we obtain from (A1.9) that

$$B = \pm 1$$

And from (A1.8), we obtain the inner and outer boundaries of the depth-of-field, R_{in} and R_{out}, as

$$R_{in} = \frac{D^2/\lambda}{1 + \frac{D^2/\lambda}{R_\varepsilon}} \qquad (4)$$

and

$$R_{out} = \frac{D^2/\lambda}{-1 + \frac{D^2/\lambda}{R_\varepsilon}} \qquad (5a)$$

which, therefore, complete the derivation of (4) and (5a).

APPENDIX II:

RESULTS OF THE ANTENNA PATTERN MEASUREMENTS

Azimuth and elevation-plane patterns, with the parabolic antenna vertically polarized, are recorded in the scales of 5°/in. and 10 dß/in.

25

$f = 9.0$ GHz
$R = 2.8$ m
Az.

76

f = 9.0 GHz
R = 2.8 m
EL.

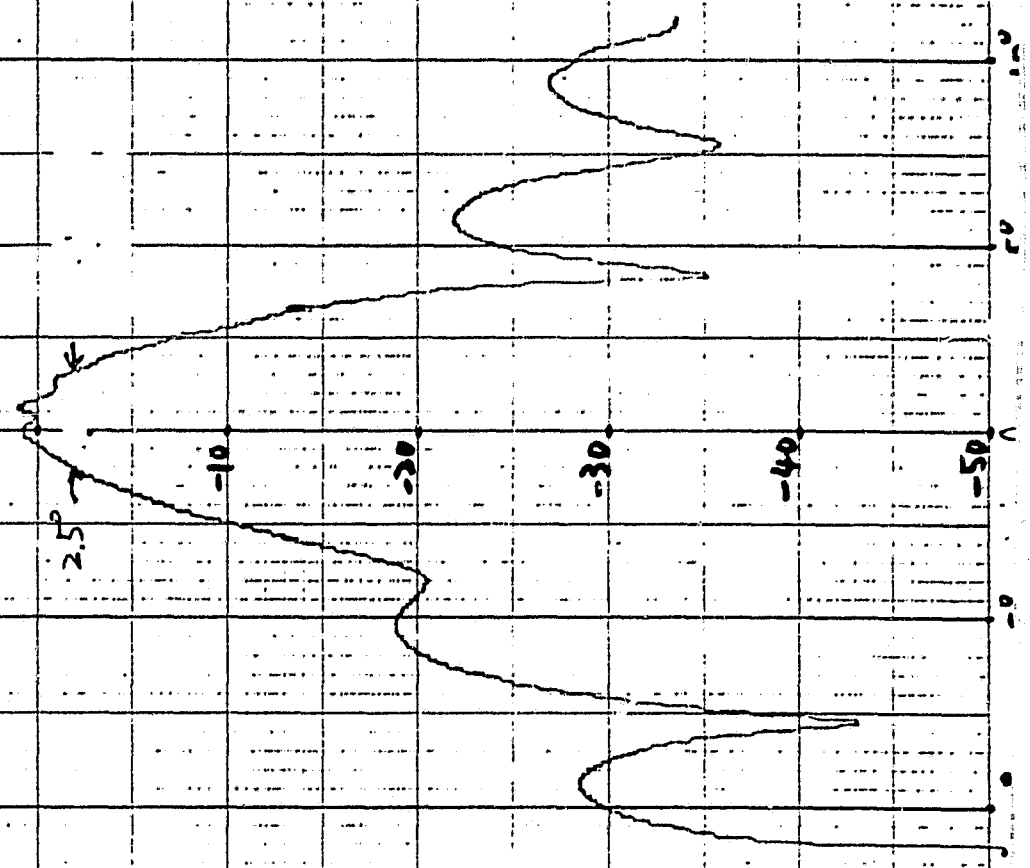

77
f = 9.0 GHz
R = 3.5 m
A2
ORIGINAL PAGE IS
OF POOR QUALITY
10°
5°
0
-10
-20
-30
-40
-50
-5.0
5°
10°

ORIGINAL PAGE IS
OF POOR QUALITY
f = 9.0 GHz
R = 3.5 m
EL.
-10
-20
-30
-40
-50
2.75°

79

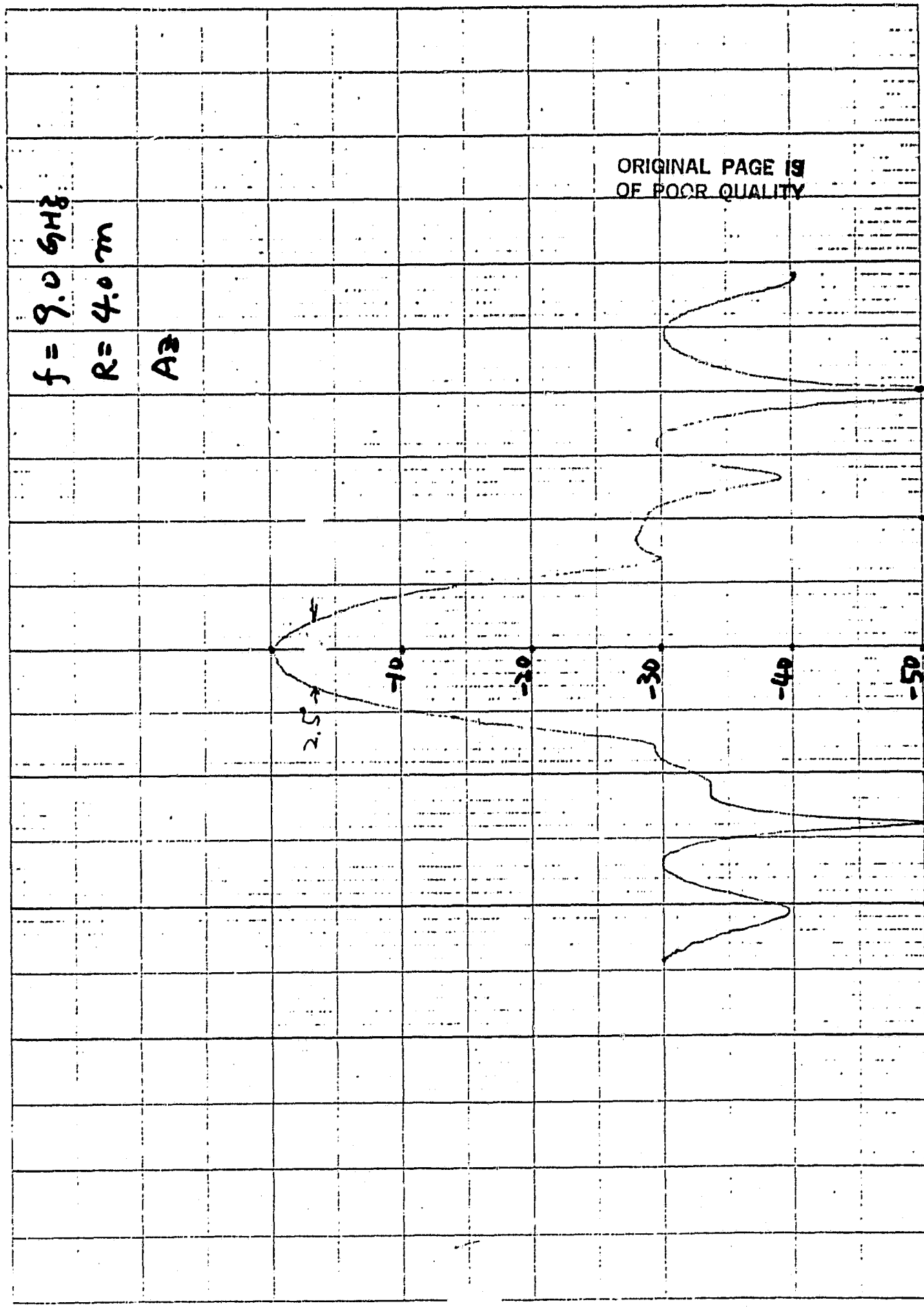
f = 9.0 GHz
R = 4.0 m
AZ
ORIGINAL PAGE IS
OF POOR QUALITY
10°
5°
0
-10
-20
-30
-40
-50
2.5°
5°
10°

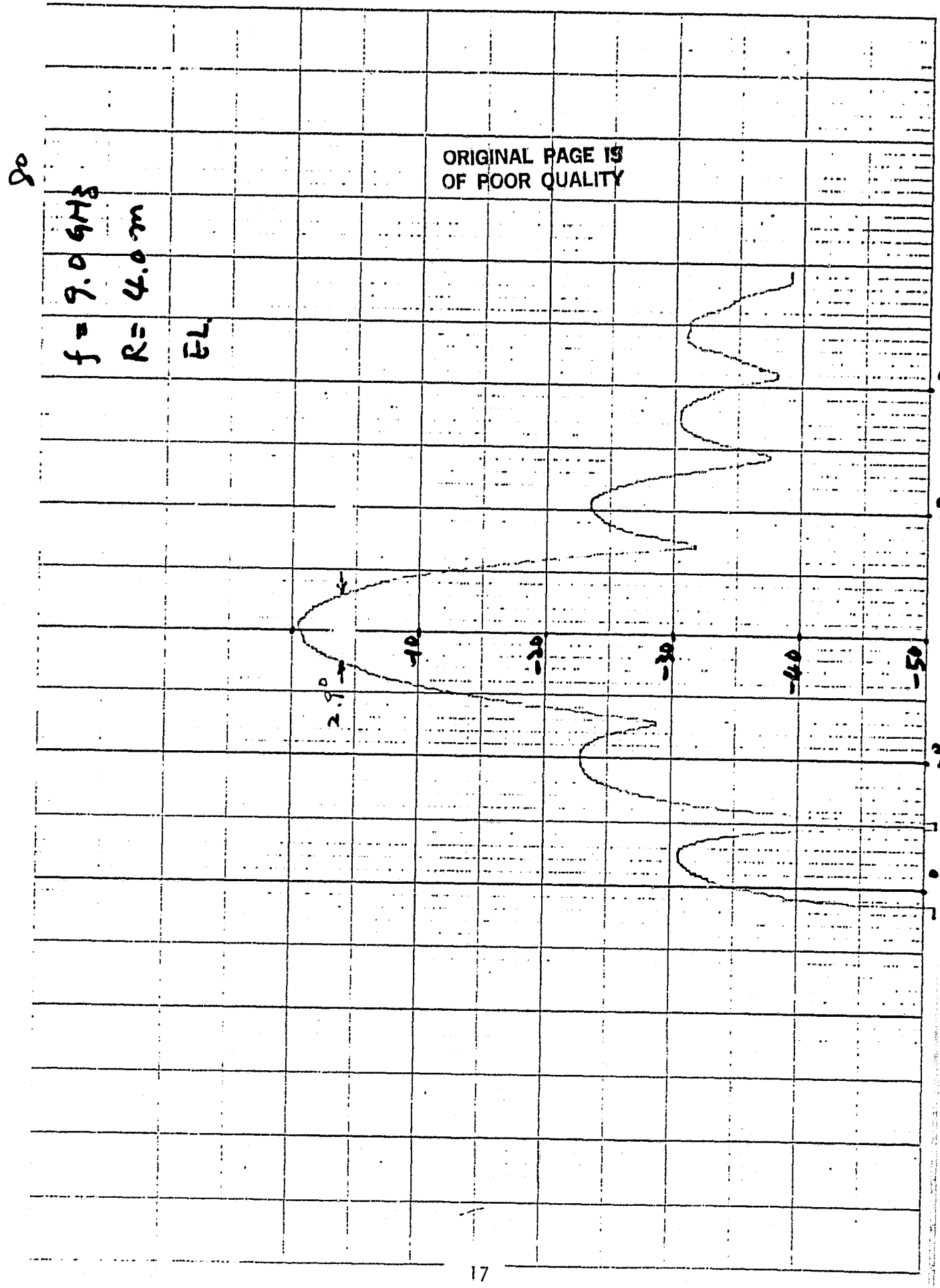
ORIGINAL PAGE IS
OF POOR QUALITY
f = 9.0 GHz
R = 4.0 m
EL
-10
-20
-30
-40
-50

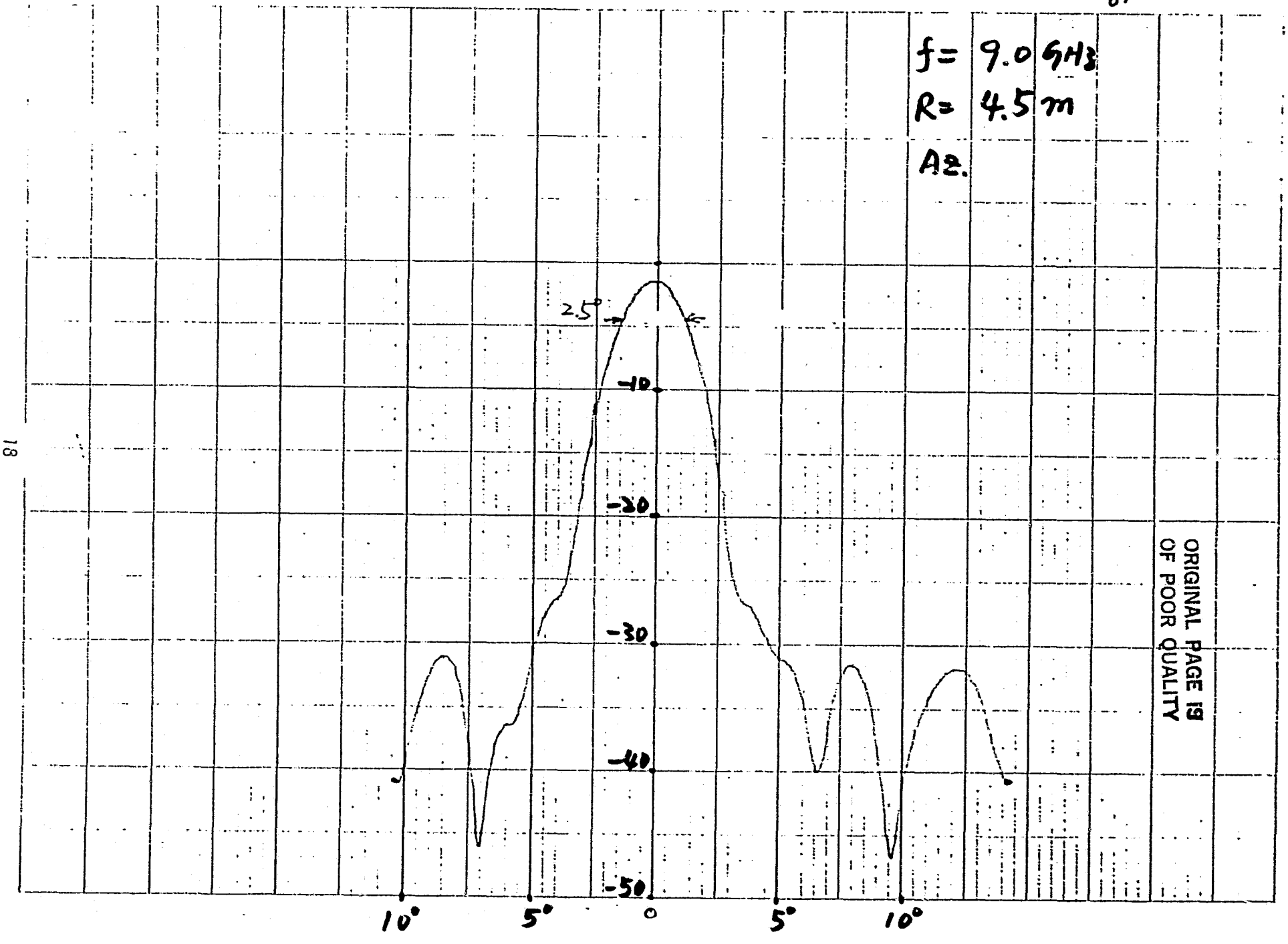

ORIGINAL PAGE IS
OF POOR QUALITY
f = 9.0 GHz
R = 4.5 m
EL.
2.6°
-10
-20
-30
-40
-50
10°
0°
-10°

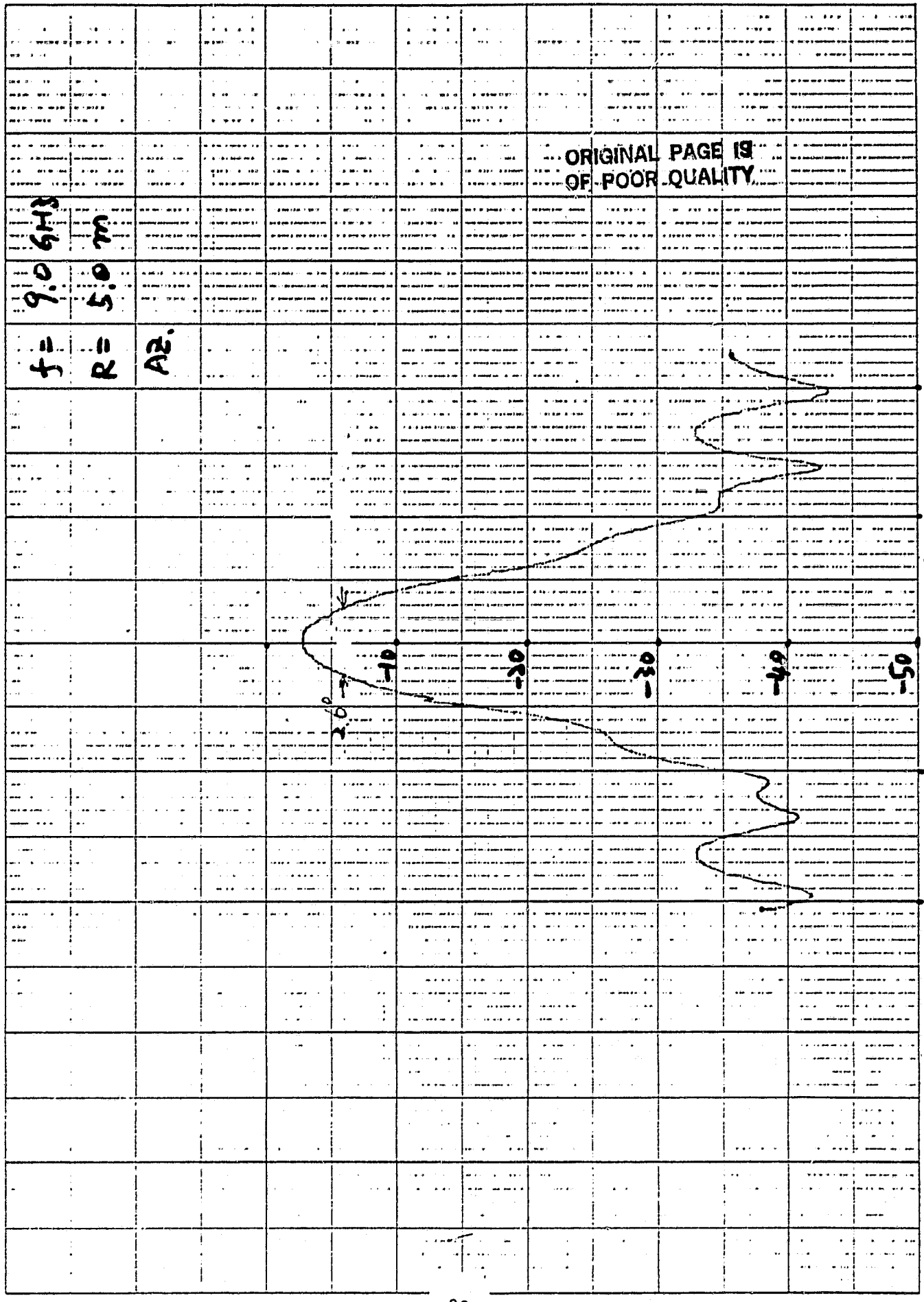

8y

f = 9.0 GHz
R = 5.0 m
Et

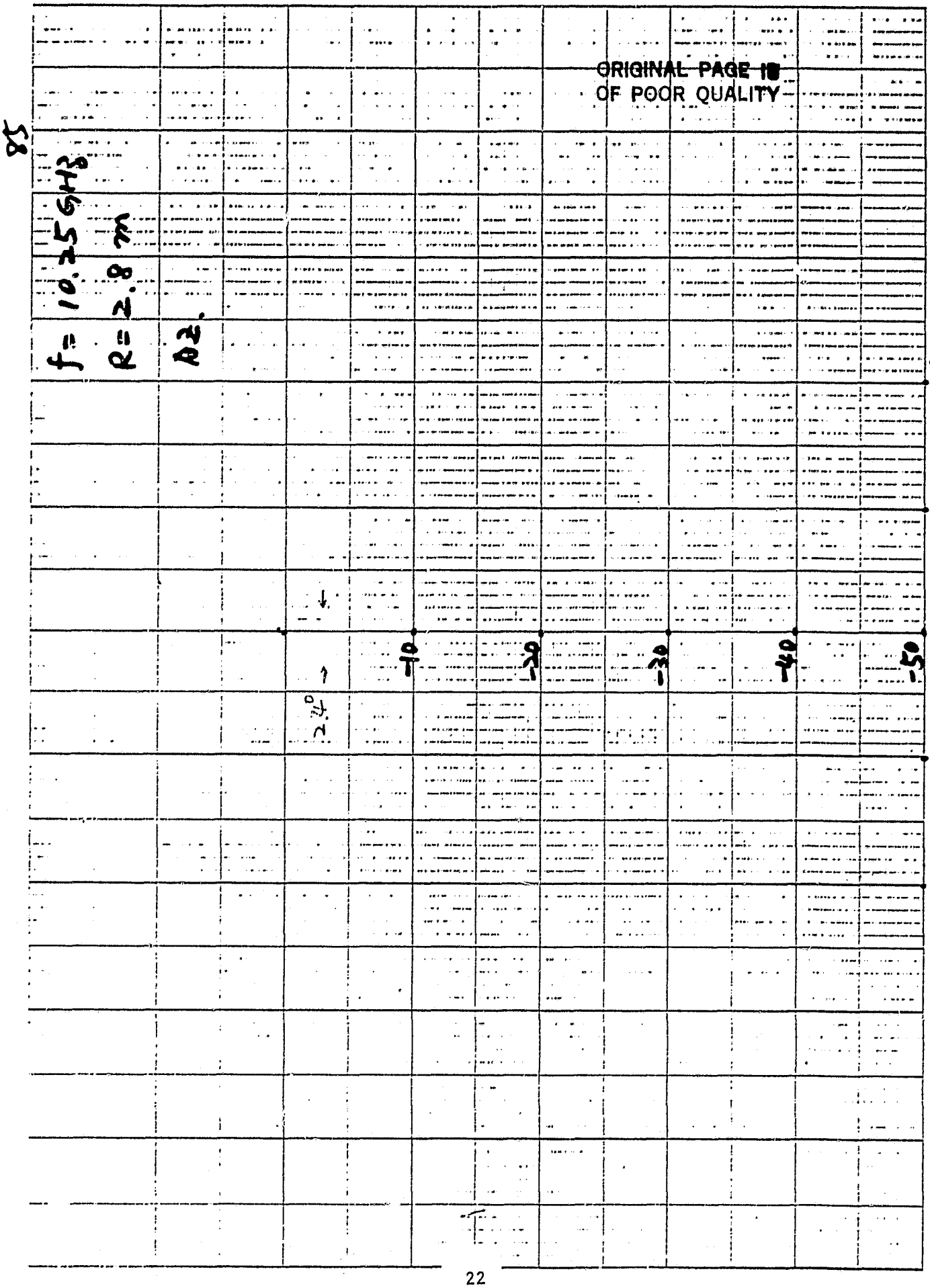

ORIGINAL PAGE IS
OF POOR QUALITY
f= 10.25 GHz
R= 2.8 m
El.
-10
-20
-30
-40
-50
23°

87

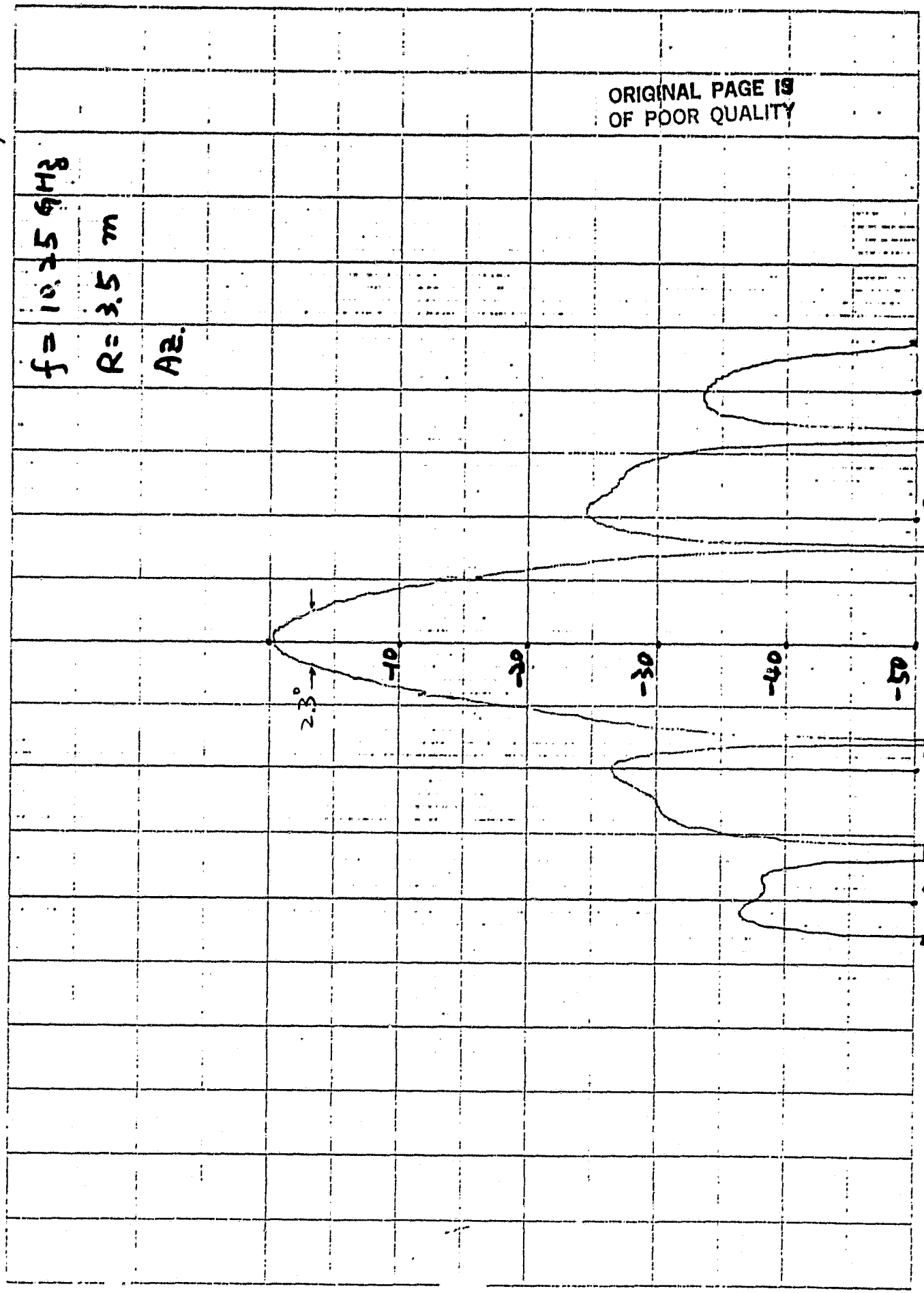

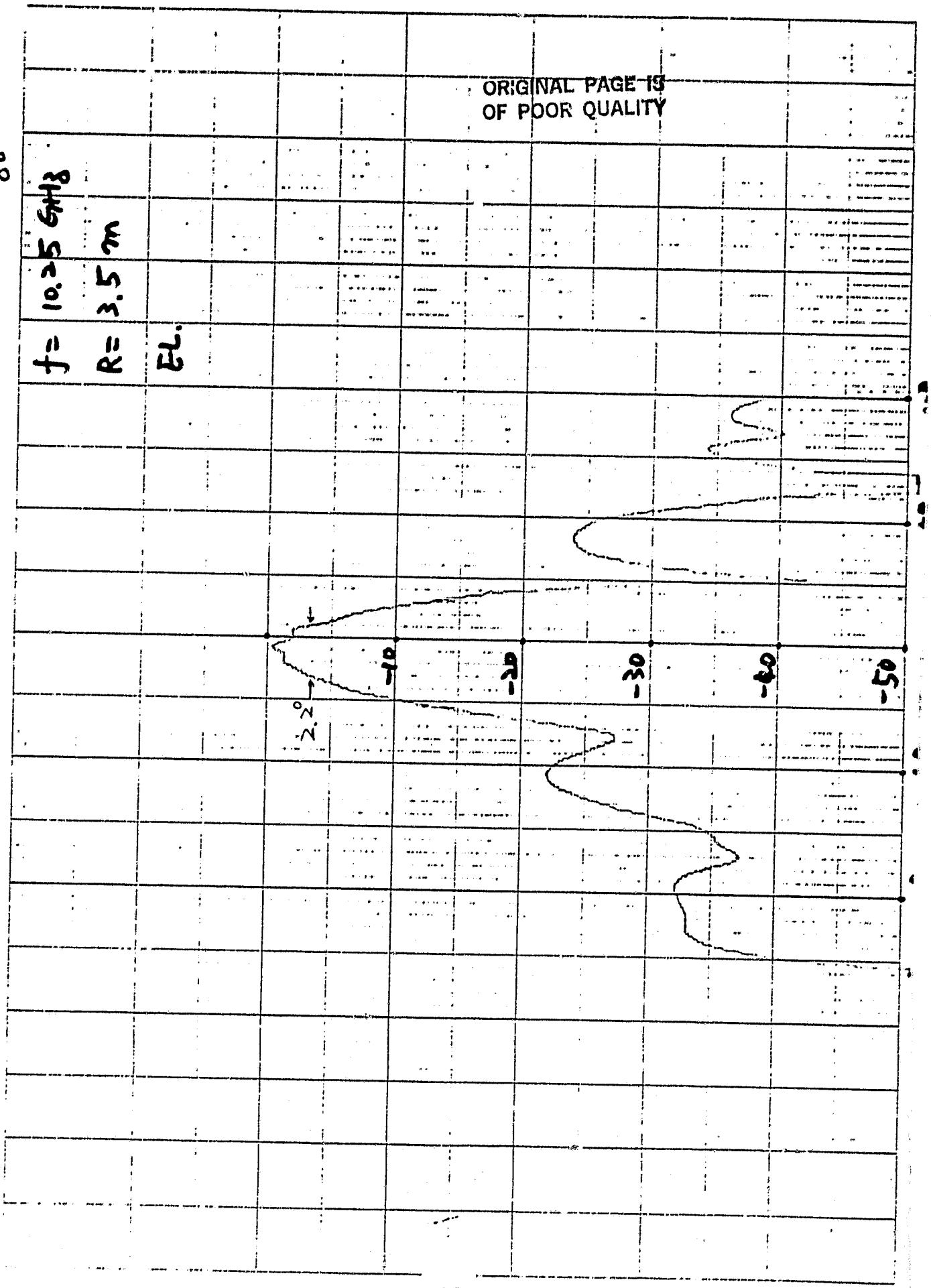

89

f= 10.25 GHz
R= 4.0m
A2.

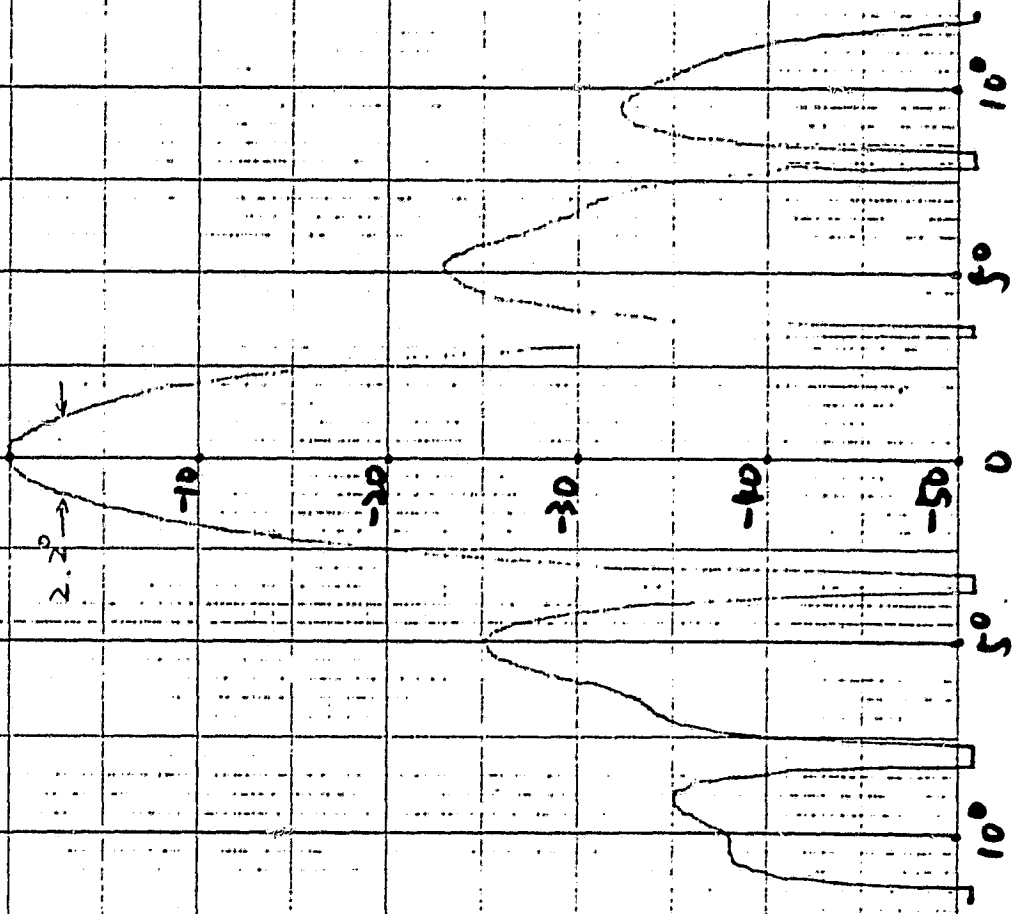

90
f= 10.25 GHz
R= 4.0 cm
EL.
ORIGINAL PAGE IS
OF POOR QUALITY
-15
-20
-30
-45
-60
2.2°

ORIGINAL PAGE IS
OF POOR QUALITY
f = 10.256 GHz
R = 4.5 m
Az
91
10°
5°
0
-10
-20
-30
-40
-50
22.5°
5°
10°

ORIGINAL PAGE IS
OF POOR QUALITY

9>

f= 10.25 GHz

R= 4.5 m

EL.

-10

-20

-30

-40

-50

2.0°

HEWLETT-PACKARD 9270 1606

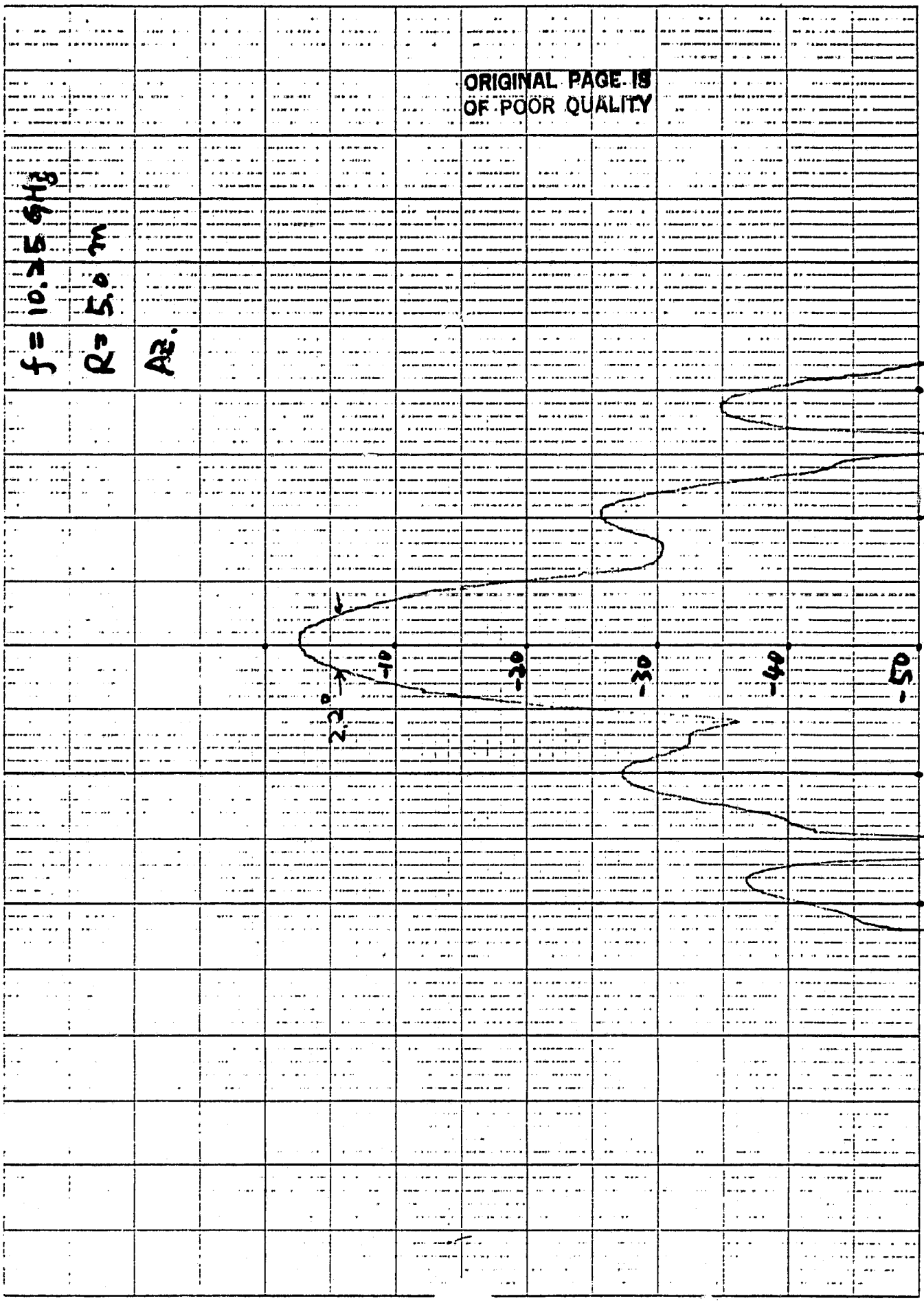

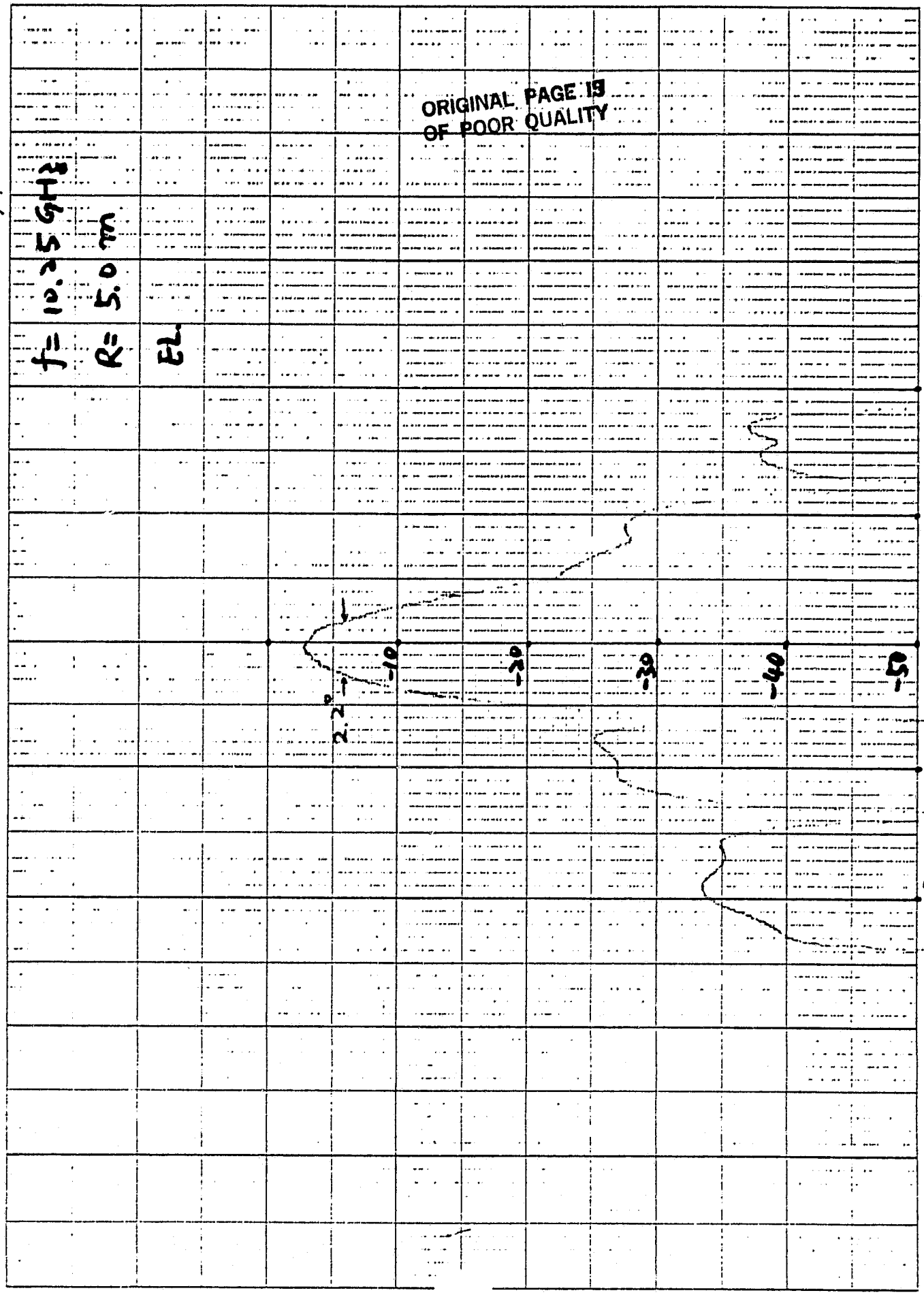

95

f = 11.5 GHz
R = 2.8 m
A3.

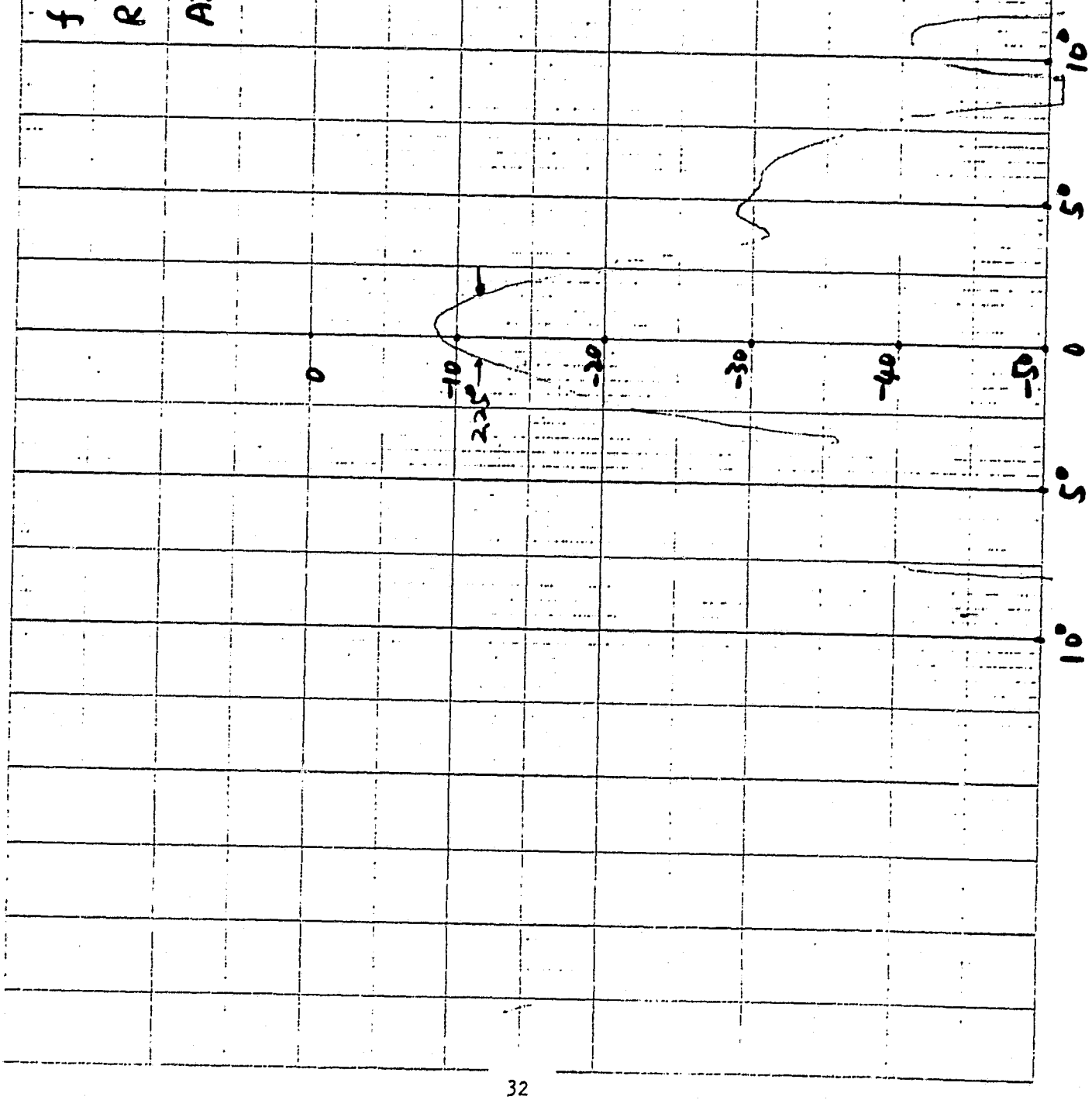

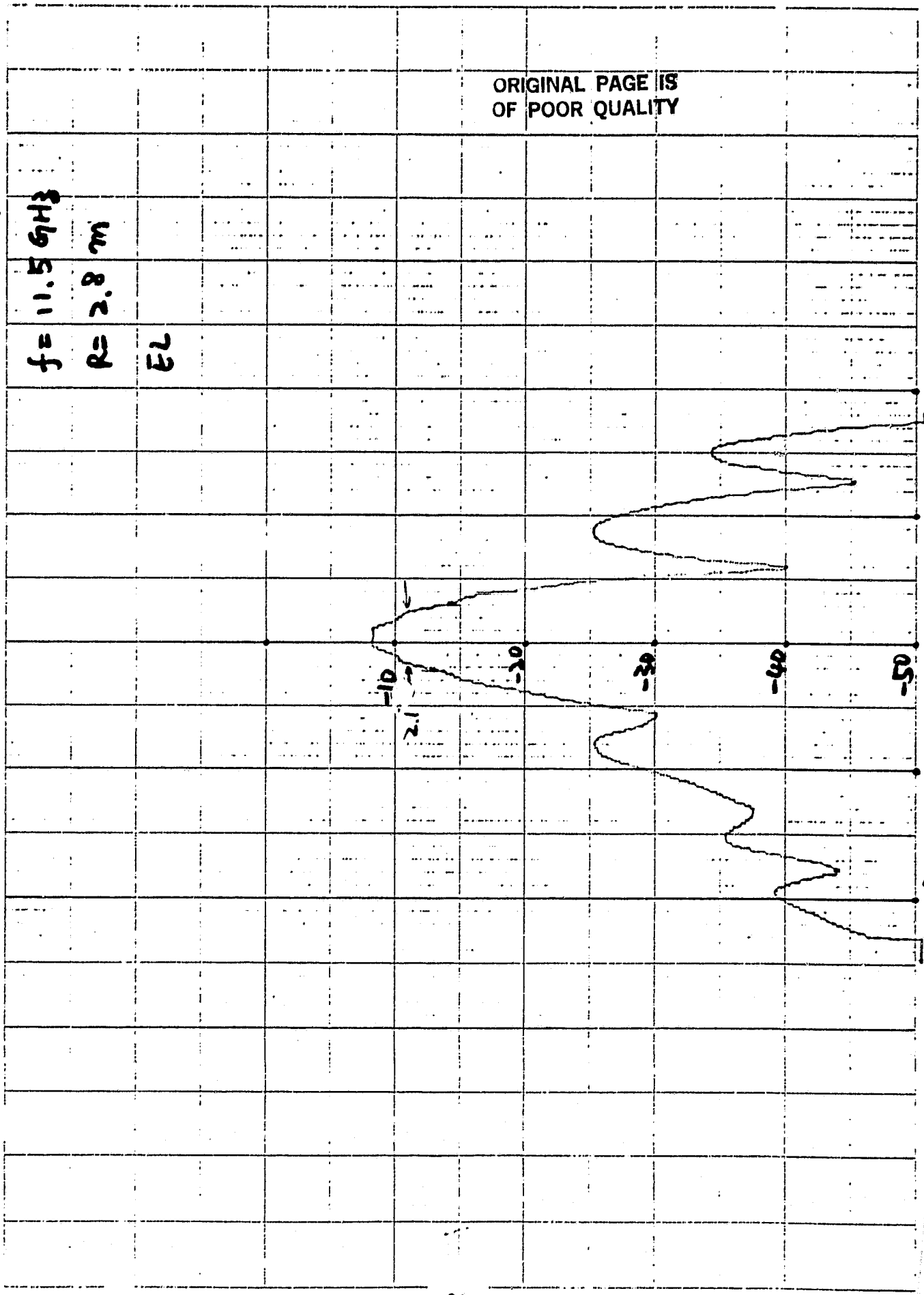
ORIGINAL PAGE IS
OF POOR QUALITY
f = 11.5 GHz
R = 2.8 m
EL
-10
-20
-30
-40
-50
10°
0°
5°
10°

97

$f = 11.5\,GHz$

$R = 3.5\,m$

A2.

78

$f = 11.5\,GHz$
$R = 3.5\,m$
EL.

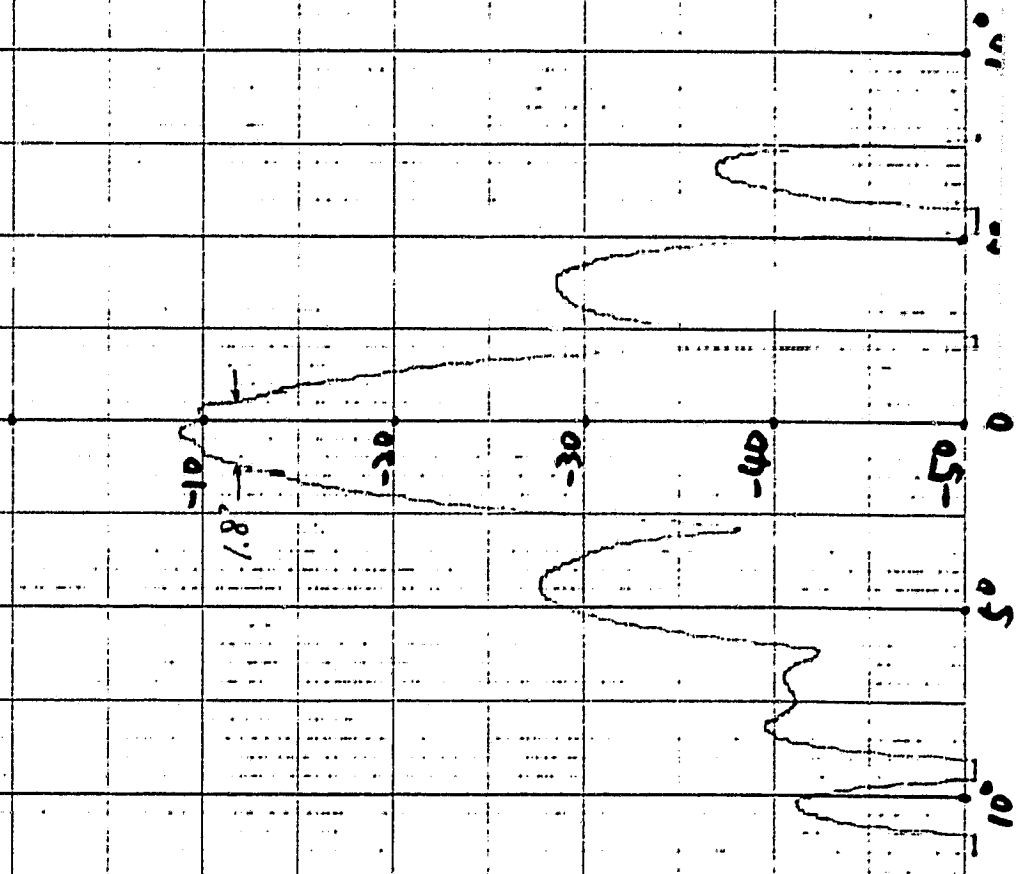

99

$f = 11.5$ GHz
$R = 4.0$ m
AZ:

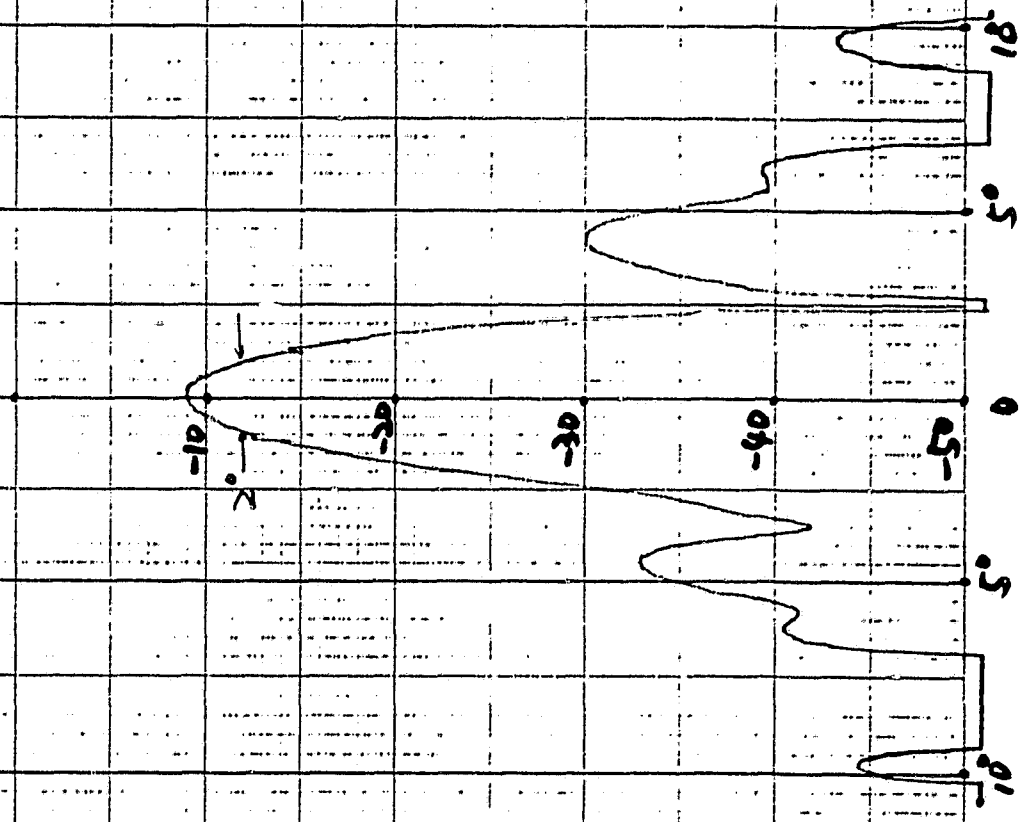

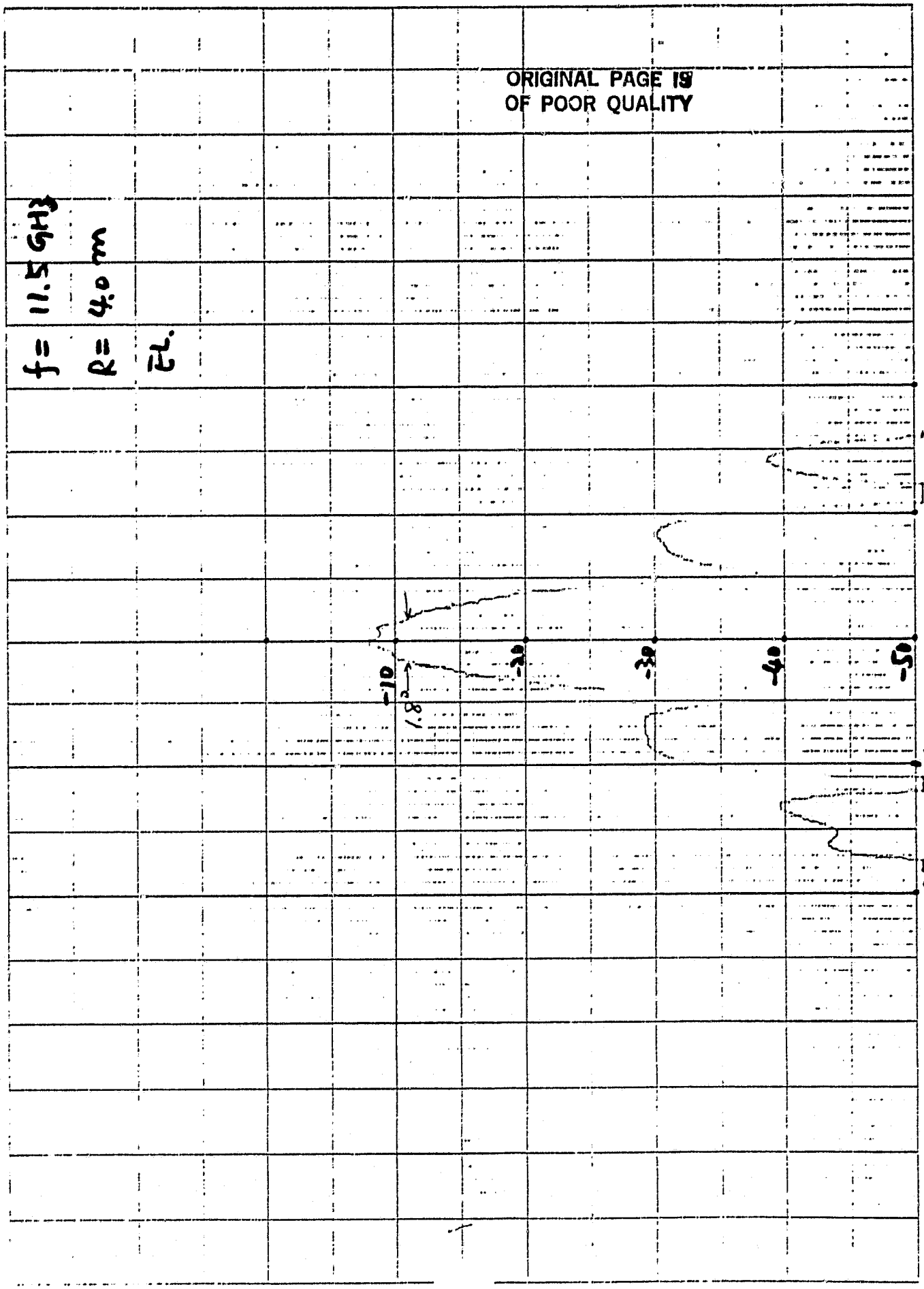

(0)

f = 11.5 GHz
R = 4.5 m
Az.

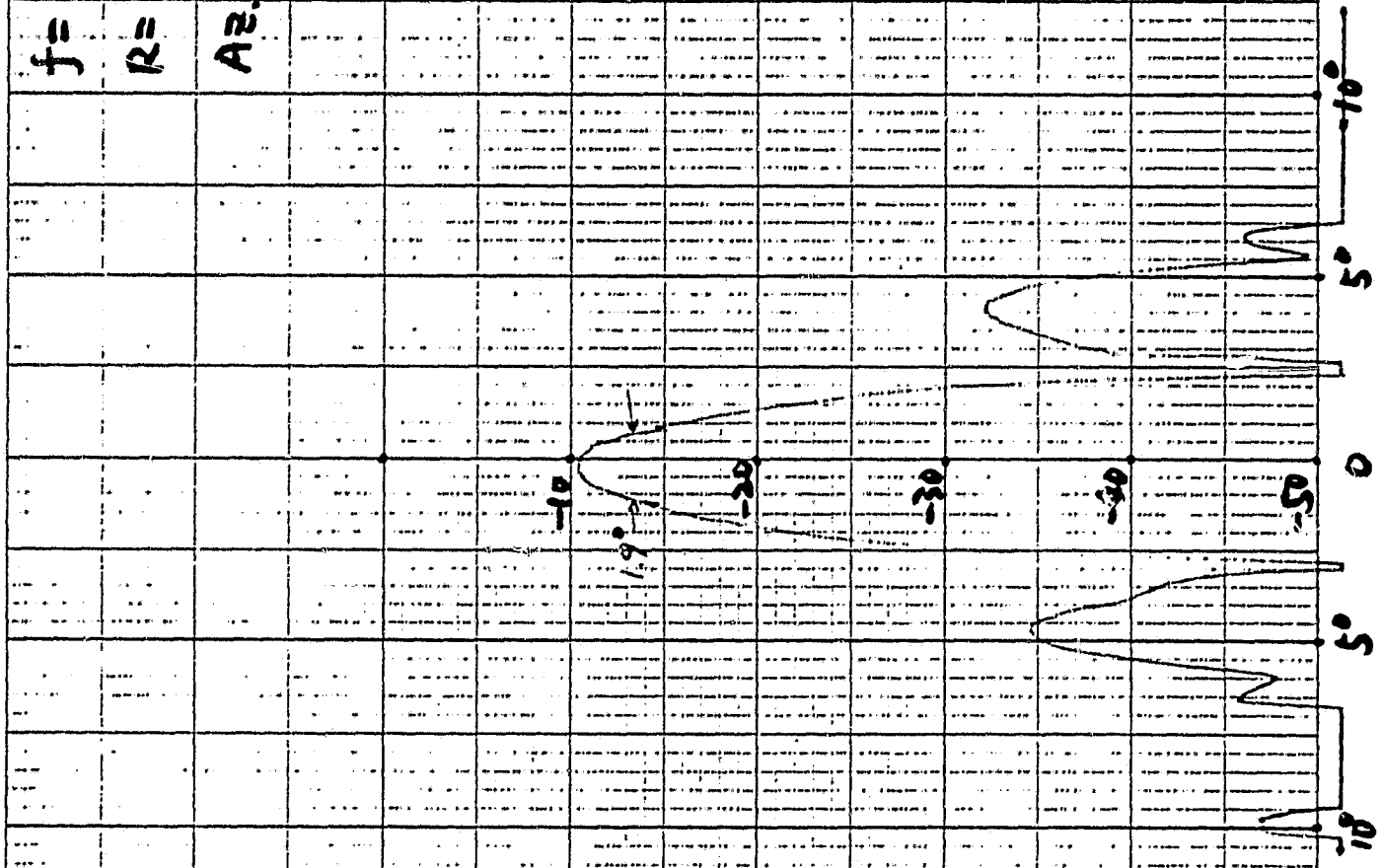

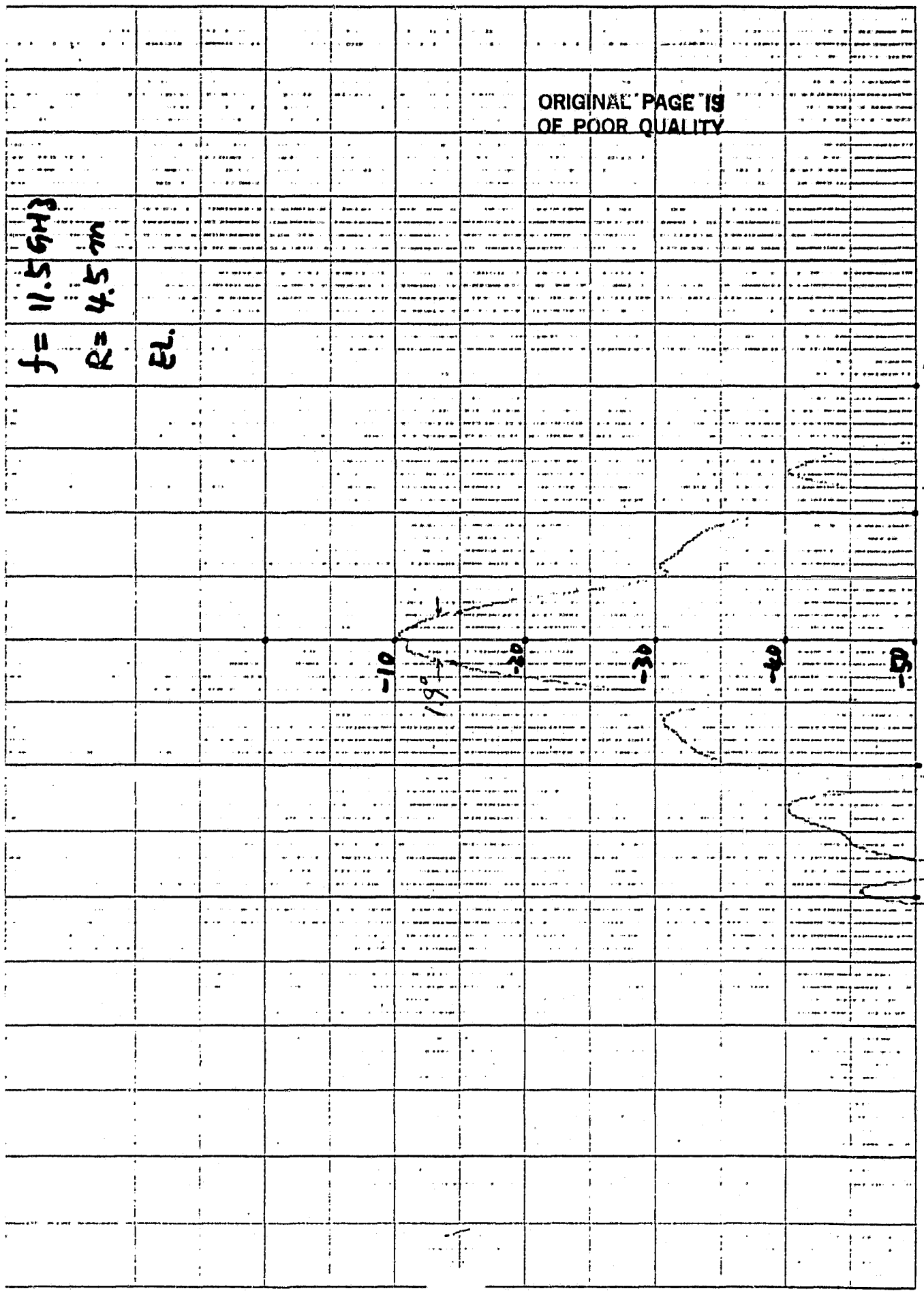

103

f = 11.5 GHz
R = 5.0 m
Az.